Electronic Supplementary Material (ESI) for New Journal of Chemistry.

Supporting Information

Hierarchical porous biochar with ultra-high specific surface area for rapid removal of antibiotics from water

Shujian Liu, Yi Wang, Zhongmin Feng, Yun Wang*, Ting Sun*

College of Sciences, Northeastern University, 3-11, Wenhua Road, Shenyang, Liaoning, 110819, China.

* Corresponding Authors: wyun1989@126.com (Yun Wang);

sun1th@163.com (Ting Sun)

Chemicals and materials

Onion skin was collected from vegetable market in Kaiyuan. Ofloxacin (OFL), norfloxacin (NOR), ciprofloxacin (CIP), sulfadiazine (SDZ), tylosin (TYL), tetracycline hydrochloride (TCH) and KOH were purchased from Shanghai Aladdin Bio-Chem Technology Co., LTD (China). Chlortetracycline hydrochloride ($C_{22}H_{23}ClN_2O_8 \cdot HCl$, CTC) and oxytetracycline hydrochloride ($C_{22}H_{24}N_2O_9 \cdot HCl$, 95%, OTC) were bought from Macklin Biochemical Co., Ltd (China). Hydrochloric acid (HCl) was obtained from Sinopharm Chemical Reagent Co., Ltd (Shanghai, China). All chemicals were analytical grade and used directly.

Characterization

The specific surface area was calculated by the Brunauer-Emmett-Teller (BET) method and the pore size distribution was analyzed using the Density Functional Theory (DFT) method. The morphology of the samples was observed by scanning electron microscopy (SEM, SU 8000, Japan) and transmission electron microscopy (TEM, G20, USA). The Raman spectra of samples were obtained by a fully automatic Raman spectrometer at a 532 nm wavelength laser (XPLORA, FRA). Moreover, the zeta potential of materials at different pH values were performed on a micro-electrophoresis apparatus (ZEN1690, UK). The functional groups of materials were evaluated using Fourier-transform infrared (FT-IR) spectroscopy (VERTEX70, Germany). X-ray photoelectron spectroscopy (XPS) was used to analyze the composition of materials (Thermo Instruments Inc, USA).

Data analysis

*SI 1.1:*The adsorption amount (Q_e) and removal rate (R (%)) of antibiotics were calculated by following equations:[1]

$$Q_t = \frac{(C_o - C_t)V}{m} \quad (1)$$

$$\text{R (\%)} = \frac{(C_o - C_t)}{C_o} \times 100\% \quad (2)$$

Where Q_t (mg/g) is the adsorption amount of adsorbents at time t (min). R (%) is the removal rate of OFL and SDZ. C_o (mg/L) is the initial concentrations of antibiotics and C_t (mg/L) is the concentrations of antibiotics at t time (min). V (mL) is the solution volume and m (mg) represents the mass of adsorbents.

SI 1.2: Kinetic modelling

Then the pseudo-first-order kinetic model (Eq. (S1)), pseudo-second-order kinetic model (Eq. (S2)) and intra-particle diffusion model (Eq. (S3)) were used to analyze the experimental data[2, 3].

$$\ln(Q_e - Q_t) = \ln Q_e - k_1 t \quad (S1)$$

$$\frac{t}{Q_t} = \frac{1}{k_2 Q_e^2} + \frac{t}{Q_e} \quad (S2)$$

$$Q_t = k_d t^{0.5} + C \quad (S3)$$

Where t is the adsorption time (min), Q_e and Q_t (mg/g) are the absorption amount of antibiotics adsorbed at equilibrium and any time t, respectively. k_1 (min^{-1}), k_2 (g/(mg·min)) and k_d (g/(mg·$h^{1/2}$)) are the adsorption rate constant of pseudo-first-order kinetic, pseudo-second-order kinetic and intraparticle diffusion models, respectively. Additionally, *C* is the intercept related to the thickness of the boundary layer.

SI 1.3: Adsorption isotherm modelling

Three isotherm models, Langmuir (Eq. (S4)), Freundlich (Eq. (S5)) and Tempkin (Eq. (S6)) were used to fit the experimental data[3, 4].

$$\frac{C_e}{Q_e} = \frac{C_e}{Q_{max}} + \frac{1}{Q_{max}K_L} \quad \text{(S4)}$$

$$\ln Q_e = \frac{1}{n}\ln C_e + \ln K_F \quad \text{(S5)}$$

$$Q_e = K_T ln C_e + K_T ln f \quad \text{(S6)}$$

Where C_e is the equilibrium concentration (mg/L), Q_e is the equilibrium absorption capacity (mg/g) and Q_{max} is the antibiotics maximum adsorption capacity (mg/g). K_L and K_F are adsorption rate constant of Langmuir and Freundlich models. K_T is Tempkin constant and f (L/mg) is Tempkin binding constant, which respectively reflect the adsorption heat and the maximum binding energy.

SI 1.4: Adsorption thermodynamics

Thermodynamic studies are used to estimate the thermodynamic parameters of antibiotic adsorption behaviour: the change of Gibbs free energy (ΔG), enthalpy (ΔH) and entropy (ΔS). The thermodynamic parameters were calculated from the following equations[5]:

$$\ln \frac{Q_e}{C_e} = -\frac{\Delta H}{RT} + \frac{\Delta S}{R} \quad \text{(S7)}$$

$$\Delta G = \Delta H - T\Delta S \quad \text{(S8)}$$

$$K_L = \frac{Q_e}{C_e}$$

Where ΔG (kJ/mol) is the Gibbs free energy change, ΔH (kJ/mol) is the enthalpy change and ΔS (J/(K·mol)) is the entropy change. R (8.314 J/(K·mol)) represents the gas constant and T (K) is the absolute temperature.

SI 2.1. The alkaline-activation mechanism

Using of KOH as an activator to activate biomass is a general but efficient method for the synthesis of active porous carbon materials with developed porosity. In general, the reaction of carbon with KOH involves the reduction of potassium (K) compounds to form metal K, oxidation of carbon to carbon oxide and carbonate, and the reaction between various active intermediates. The reaction equation can be expressed as follows[6]:

$$6KOH + 2C \rightarrow 2K + 3H_2 + 2K_2CO_3 \quad (1)$$

$$K_2CO_3 \rightarrow K_2O + CO_2 \quad (2)$$

$$CO_2 + C \rightarrow 2CO \quad (3)$$

$$K_2CO_3 + 2C \rightarrow 2K + 3CO \quad (4)$$

$$C + K_2O \rightarrow 2K + CO \quad (5)$$

During the KOH activation process, previous results indicated that K_2CO_3 formed at about 400 C, and at about 600℃, KOH is completely depleted (Eqn. (1))[7]. The K_2CO_3 formed during the reaction decomposes into CO_2 and K_2O at a temperature exceeds 700°C, and disappears completely at 800°C (Eqn. (2)). From Eqn. (3) we can see that, the resulting CO_2 can be further reduced by carbon to form CO at high temperature. The compounds of metal K (K_2O and K_2CO_3) can also be reduced by carbon to form metal K at temperatures exceeding 700℃[8].

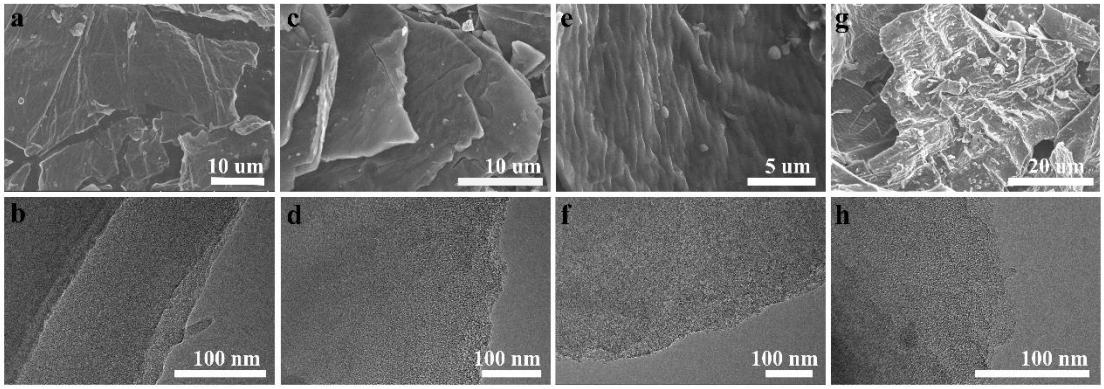

Fig. S1 SEM and TEM images of samples with different immersion ratios: (a), (b) OPBC; (c), (d) OHPBC-3; (e), (f) OHPBC-4; (g), (h) OHPBC-6.

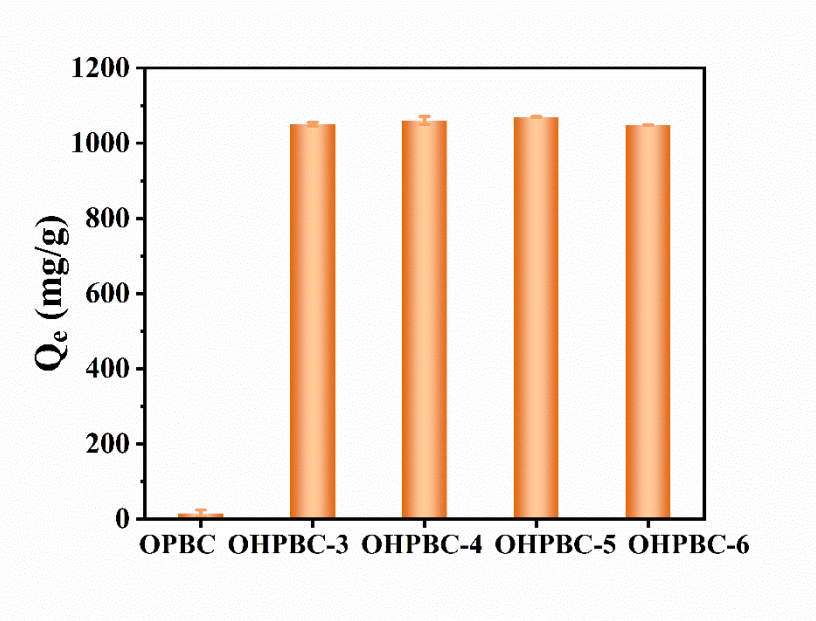

Fig. S2 The adsorption capacity of ofloxacin (OFL) on OHPBCs and OPBC

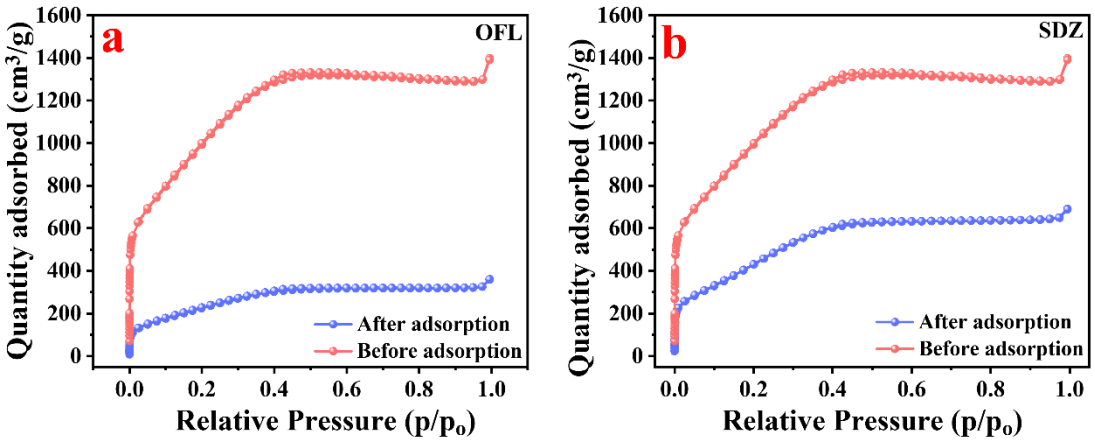

Fig. S3 N_2 adsorption/desorption isotherms before and after (a) LFC and (b) SDZ adsorption onto OHPBC-5.

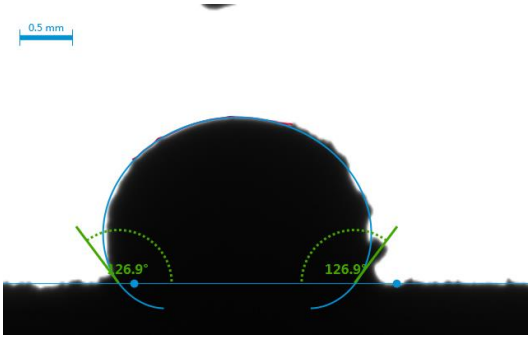

Fig S4 Contact angle measurement of the OHPBC-5.

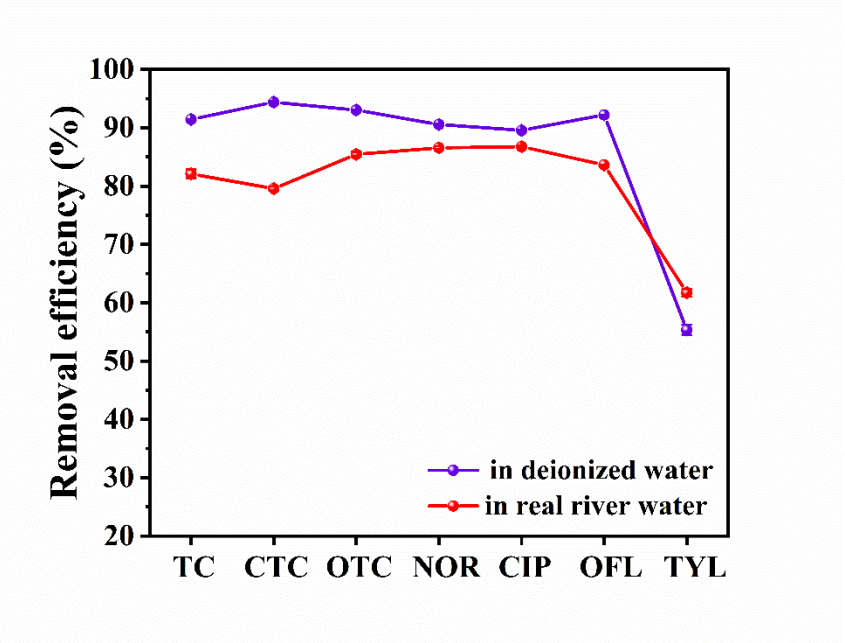

Fig. S5 The removal efficiency of different antibiotics in deionized water and real river water.

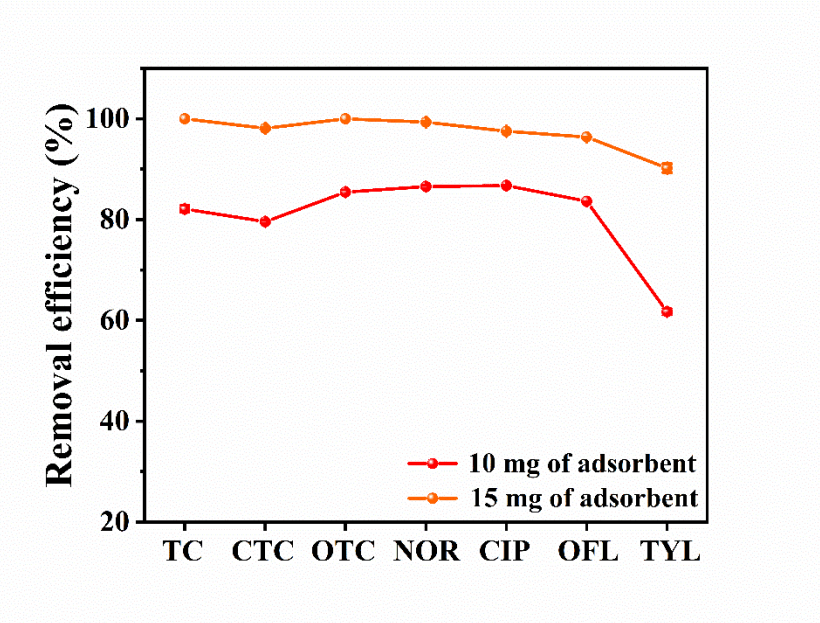

Fig. S6 Effect of adsorbent dosage on the removal efficiency of different antibiotics in real river water.

Table S1 Surface areas and pore volume of OPBC and OHPBCs

Sample	OPBC	OHPBC-3	OHPBC-4	OHPBC-5	OHPBC-6
S_{BET}(m^2/g)	137.6	2917.4	3503.3	3787.6	3201.4
Pore volume (cm^3/g)	0.071	1.31	1.54	1.95	1.82

Table S2 Comparison of adsorption capacity and adsorption time of various adsorbents for OFL and SDZ.

	Adsorbents	S_{BET} (m^2/g)	Q_m (mg/g)	Adsorption conditions	Equilibration time (min)	Ref
OFL	Chitosan/reed biochar composite	141.0	6.64	C_o=4-20mg/L, 298 K	1200	9
	Sludge biochar (BTSFe)	91	17.9	C_o=30-300 mg/L, 298 K	300	10
	(Fe/Zn + H_3PO_4) modified sludge biochar	39.1	25.4	C_o=5-100 mg/L, 298 K	720	11
	Loofah sponge-derived activated carbon	834.	131.93	C_o=20-80 mg/L, 298 K	240	12
	MIL-101(Cr)-SO_3H	1760	450.4	C_o=20-100 mg/L, 303 K	1440	1
	ZIF-8	650.8	194.1	C_o=5-100 mg/L, 298 K	120	13
SDZ	glucose-based mesoporous carbon	1126.5	246.73	C_o=10-100 mg/L, 308K	120	14
	cotton shells biochar	1225.6	86.89	C_o=10-100 mg/L, 298K	720	15
	Olive pomace-derived biochar	2451.8	66.2252	C_o=5-50 mg/L, 298 k	120	16
	Amino-functionalized porous carbon	1164	90.7	C_o=1-20 mg/L, 298K	720	17
	Pinewood-derived porous biochar	738	261	C_o=6-48 mg/L, 298 K	2880	18
	hydroxylated multi - walled carbon nanotubes	105.07	132.334	C_o=10-100 mg/L,298 K	20	19
OFL	**This study (OHPBC-5)**	**3787.6**	**1134.76**	**C_o=10-60 mg/L, 298 K**	**10**	
SDZ	**This study (OHPBC-5)**	**3787.6**	**1281.25**	**C_o=10-60 mg/L, 298 K**	**10**	

Table S3 Kinetic parameters for the adsorption of OFL and SDZ onto the OHPBC-5

			OFL			SDZ		
Kinetic model		Parameters	20 mg/L	30 mg/L	40 mg/L	20 mg/L	30 mg/L	40 mg/L
Pseudo-first-order		k_1	0.189	0.291	0.248	0.298	0.218	0.284
		R^2	0.974	0.972	0.976	0.966	0.962	0.878
Pseudo-second-order		Q_{exp} (mg/g)	911.448	1058.097	1123.092	732.813	914.882	1048.528
		Q_{cal} (mg/g)	925.93	1080.83	1137.73	740.74	925.93	1065.65
		k_2 (g/mg)	2.05×10^{-3}	2.28×10^{-3}	3.34×10^{-3}	4.38×10^{-3}	3.73×10^{-3}	3.71×10^{-3}
		R^2	0.999	0.999	0.999	0.999	0.999	0.999
Intra-particle diffusion model	Step1	$k_{d,1}$ (mg/ ($g^1\cdot h^{1/2}$))	179.94	252.38	187.94	117.57	139.39	181.55
		C_1	468.95	533.61	736.59	460.81	610.90	671.89
		R^2	0.987	0.987	0.950	0.998	0.976	0.996
	Step2	$k_{d,2}$ (mg/ ($g^1\cdot h^{1/2}$))	83.46	27.95	38.14	42.50	45.03	71.12
		C_2	634.88	932.59	994.84	596.62	775.88	865.32
		R^2	0.995	0.878	0.987	0.972	0.977	0.949
	Step3	$k_{d,3}$ (mg/ ($g^1\cdot h^{1/2}$))	23.78	12.46	8.66	7.73	13.29	0.74
		C_3	806.28	1002.52	1085.3	697.21	857.25	1045.24
		R^2	0.975	0.953	0.941	0.927	0.977	0.935

Table S4 Fitting parameters of three isotherm models for OFL and SDZ adsorption onto OHPBC-5.

Adsorbates	Langmuir			Freundlich			Tempkin		
	K_L ($L \cdot mg^{-1}$)	Q_{max} ($mg \cdot g^{-1}$)	R^2	K_F	n	R^2	K_T ($L\ mg^{-1}$)	*f*	R^2
OFL	1.91	1134.76	0.995	625.9	4.53	0.925	175.24	42.52	0.98
SDZ	0.30	1281.25	0.997	382.36	2.96	0.97	247.54	3.42	0.99

Table S5 Thermodynamic parameters for OFL and SDZ adsorption on OHPBC-5.

Antibiotics	T (K)	K_L	△G (kJ/mol)	△H (kJ/mol)	△S (J/(K·mol))
OFL	298	289.11	-14.03	-5.37	29.2
	308	274.84	-14.38		
	318	252.64	-14.63		
SDZ	298	120.83	-11.88	-25.09	-44.31
	308	88.55	-11.45		
	318	62.08	-10.98		

Table S6 Physiochemical properties of the studied OFL and SDZ.

	Formula	Structure	pk_{a1}	pk_{a2}	Molecular weight	Ref.
OFL	$C_{18}H_{20}FN_3O_4$	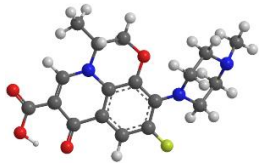	6.08	8.28	361.37	[20]
SDZ	$C_{10}H_{10}N_4O_2S$	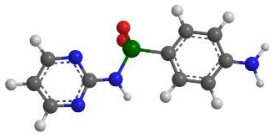	1.57	6.5	250.28	[21]

Table S7 The XPS element analysis of OHPBC-5 before and after adsorption.

Samples						C 1s (%)		
	C (%)	O (%)	N (%)	F (%)	S (%)	C-C/C=C	C-O	C=O
OHPBC-5	6.3	93.02				0.56	0.25	0.19
OFL-OHPBC-5	10.01	85.52	3.3.	1.18		0.52	0.37	0.11
SDZ-OHPBC-5	7.53	85.64	5.51		1.32	0.51	0.29	0.20

Table S8 Changes of specific surface area and pore volume of OHPBC-5 before and after adsorption.

Sample	After adsorption of OFL	After adsorption of SDZ
S_{BET}(m^2/g)	893.1	1843.4
Pore volume (cm^3/g)	0.45	0.91

References

1. X. Y. Guo, C. F. Kang, H. L. Huang, Y. J. Chang and C. L. Zhong, *Micropor. Mesopor. Mat.*, 2019, **286**, 84-91.

2. H. T. Fan, W. Sun, B. Jiang, Q. J. Wang, D. W. Li, C. C. Huang, K. J. Wang, Z. G. Zhang and W. X. Li, *Chem. Eng. J.*, 2016, **286**, 128-138..

3. C. H. Liang, X. D. Zhang, P. Feng, H. X. Chai and Y. M. Huang, *Chem. Eng. J.*, 2018, **344**, 95-104.

4. H. M. Jang, S. Yoo, Y. K. Choi, S. Park and E. Kan, *Bioresour. Technol.*, 2018, **259**, 24-31.

5. Z. H. Yang, J. Cao, Y. P. Chen, X. Li, W. P. Xiong, Y. Y. Zhou, C. Y. Zhou, R. Xu and Y. R. Zhang, *Micropor. Mesopor. Mat.*, 2019, **277**, 277-285.

6. J. Wang and S. Kaskel, *J. Mater. Chem.*, 2012, **22**, 23710-23725.

7. E. Raymundo-Piñero, P. Azaïs, T. Cacciaguerra, D. Cazorla-Amorós, A. Linares-Solano and F. Béguin, *Carbon.*, 2005, **43**, 786-795.

8. G. Singh, K. S. Lakhi, S. Sil, S. V. Bhosale, I. Kim, K. Albahily and A. Vinu, *Carbon.*, 2019, **148**, 164-186.

9. C. Zhu, Y. Lang, B. Liu and H. Zhao, *Polycycl. Aromat. Comp.*, 2018, **39**, 287-297.

10. V. Singh and V. C. Srivastava, *Environ. Pollut.*, 2020, **259**, 113822.

11. Y. F. Ma, P. Li, L. Yang, L. Wu, L. Y. He, F. Gao, X. B. Qi and Z. L. Zhang, *Ecotox. Environ. Safe.*, 2020, **196**, 110550.

12. Q. Kong, X. He, L. Shu and M. S. Miao, *Process Saf. Environ.*, 2017, **112**, 254-

264..

13. R. B. Yu and Z. C. Wu, *Micropor. Mesopor. Mat.*, 2020, **308**, 110494.

14. B. Wang, X. Y. Xu, H. Tang, Y. L. Mao, H. H. Chen and F. Y. Ji, *Appl. Surf. Sci.*, 2020, **528**, 147048.

15. Q. M. Meng, Y. L. Zhang, D. Meng, X. P. Liu, Z. J. Zhang, P. L. Gao, A. G. Lin and L. Hou, *Environ. Res.*, 2020, **191**, 110104.

16. S. Aslan and M. Şirazi, *Water. Air. Soil. Poll.*, 2020, **231**, 222.

17. Y. Wang, W. B. Jiao, J. T. Wang, G. F. Liu, H. L. Cao and J. Lu, *Bioresour. Technol.*, 2019, **277**, 128-135.

18. C. Y. Li, X. X. Zhu, H. L. He, Y. X. Fang, H. P. Dong, J. H. Lü, J. F. Li and Y. M. Li, *J. Mol. Liq.*, 2019, **274**, 353-361.

19. Y. B. Liu, Y. L. Peng, B. H. An, L. C. Li and Y. Liu, *Chemosphere.*, 2020, **246**, 125778.

20. R. S. Bangari and N. Sinha, *J. Mol. Liq.*, 2019, **293**, 111376.

21. M. Jiang, W. B. Yang, Z. W. Zhang, Z. Yang and Y. P. Wang, *J. Environ. Sci.*, 2015, **31**, 226-234.